Catalysis Letters 62 (1999) 1–13

Perspectives in Catalysis

What do we know about the acidity of solid acids? [*]

R.J. Gorte

Department of Chemical Engineering, University of Pennsylvania, Philadelphia, PA 19104, USA

Received 1 June 1999; accepted 21 June 1999

With a proper understanding of the nature of solid acidity, zeolites and other solid acids have great potential for replacing homogeneous acids in a wide range of catalytic applications. This paper describes results from our laboratory on the characterization and description of the acid sites in high-silica zeolites, especially H-MFI. A crucial observation from this work is the identification of stoichiometric adsorption complexes, one molecule per framework Al, for a wide range of adsorbates, including amines, alcohols, nitriles, ketones, and thiols. Examples are given in which temperature-programmed desorption is used to identify these complexes and characterize their initial chemistries. Calorimetric measurements on the 1 : 1 complexes have been used to compare the enthalpies of protonation in the zeolite to enthalpies of protonation in the gas phase and in aqueous phase and to demonstrate that a gas-phase basis provides better predictive capabilities. The issue of carbenium-ion stabilities is discussed, as well as the unusual catalytic properties of acid sites formed by framework substitution of Fe. The effect of sorption and cavity size on reactions is described. Finally, the problems associated with trying to define or characterize solid acids by using ammonia TPD or ^{13}C NMR isotropic shifts of ketones without proper consideration of the complicated nature of these techniques are discussed.

Keywords: acid catalysis, zeolites, temperature-programmed desorption, microcalorimetry, NMR

1. Introduction

Acid-catalyzed reactions are among the most important industrial reactions. While there are significant advantages to practicing these reactions over solid acids, most processes continue to use liquid-phase acids. With only a relatively few important exceptions, attempts to replace homogeneous acids with their heterogeneous counterparts have not been successful. There are many reasons why solid acids have not been used more often. However, it is my belief that solid acids, especially zeolites, would be used much more frequently if we had a better understanding of acidity in solids and if we were better able to quantify and describe solid acidity. This has been the overall goal of the zeolite work in which my collaborators and I have been engaged over the last 15 years [1,2].

In this paper, I will start by discussing the viewpoint we have taken on our research of zeolite acidity. Because the question of site concentrations is so crucial to any measurement on solid acids, I will next focus on methods for measuring Brønsted-acid site densities and the influence of adsorbate coverages on spectroscopic measurements. Finally, I will discuss our attempts to describe adsorption complexes and their influence on reaction chemistry.

2. Initial remarks about solid acids

Most of our research has focussed on understanding Brønsted-acid sites, which are generated as a result of protons balancing the charge associated with framework substitution of Al^{3+} for Si^{4+}, since it is generally accepted that these sites are required for many of the most important reactions [3]. Furthermore, most of our work has focussed on high-silica, unsteamed zeolites. There are several important reasons to concentrate on high-silica materials with no extra-framework Al. First, the acid sites are isolated and relatively non-interacting. Second, the pioneering work of Haag and coworkers at Mobil has shown that the activities for a large number of reactions increase linearly with Al content [4–6]. In the case of H-MFI (also known as H-ZSM-5), poisoning with alkali cations also decreases activity in a one-for-one manner (one cation poisons one site), which is strong evidence that all Brønsted sites have identical activity [6]. Finally, since materials with higher Al contents, such as faujasite (FAU) hydrocarbon-cracking catalysts, are rapidly steamed to high-silica materials in actual use, it does not appear worthwhile to focus too much attention on the initial, high-alumina materials.

A formal, quantitative discussion of acid–base interactions is given elsewhere [1]. A most important point from that discussion is that, in acid solutions, solvation effects are as important in determining the enthalpy and free energy of the acid–base interaction as are the actual proton-transfer steps. While reactions carried out on solid acids may result in the same products as those carried out in solution phase, there is no reason to expect that the energies of species formed along a given reaction coordinate should scale with solution-phase energies. Therefore, attempts to describe acidity by solution-phase analogies will be inappropriate. We should not expect that it will be possible to describe "acid strength" in terms of a single number, like Hammett acidity, any more than we could describe the

---

[*] This paper is based on the 1999 Emmett Award lecture presented at the North American Catalysis Society Meeting.

"hydrogenation activity" of a Pt catalyst by a single number.

In the same manner, frequently heard statements, such as "zeolites are not acidic enough for certain reactions" and "zeolites are not superacids", are not helpful for predicting chemistry and simply lead to confusion. These statements cause many to make the inappropriate comparison of zeolite acid sites to solution-phase acids and are therefore misleading. For example, recent estimates of the proton affinity of the zeolite framework anion place it below 1200 kJ/mol [7]. This value is lower than the proton affinity of conjugate anions corresponding to very strong acids, like $CF_3SO_3^-$ (1280 kJ/mol), HSO_4^- (1296 kJ/mol), and I^- (1312 kJ/mol), and CF_3COO^- (1351 kJ/mol) [8]. On this basis, one might indeed characterize zeolites as superacids. More important, statements comparing zeolites to solution-phase acids prevent one from considering conditions which might allow the use of zeolite catalysts. For example, the apparently low activity of acidic zeolites for some reactions is sometimes due to strong interactions of reactant or product molecules with the sites, not to the inability of the zeolite to protonate reactants. In the acylation of benzene with acetic acid over an acidic zeolite, it was shown that the strong adsorption of acetic acid, which is not normally considered to be a strong base, prevents adsorption of benzene [9]. The isomerization of butene is another example where simple reaction studies can be misleading. This reaction does not proceed at room temperature due to rapid oligomerization of butene at the acid sites, not because zeolites are unable to protonate small olefins [10].

By considering only high-silica, unsteamed zeolites, I will intentionally avoid questions associated with the super activity for hydrocarbon cracking found with steamed zeolites and with sulfated zirconias. In the case of sulfated zirconias, it seems clear that the high activity is associated with the fact that these materials have both Brønsted sites and redox sites [11]. Recognition of this fact will change how one attempts to use this material and how one attempts to modify zeolites to carry out similar reactions. Regarding steamed zeolites, we found no evidence in our work that an ultrastable Y zeolite (USY) is more able to protonate ethylene or propylene than a chemically dealuminated H-Y having the same framework Al content [12]. We concluded that hydrocarbon-cracking activity is significantly higher on the USY, not because of enhanced acidity, but rather because of the complexity of hydrocarbon cracking [12,13], a conclusion reinforced by recent results from Northwestern University [14].

3. Site densities

Before one can begin to describe the reactions which occur at Brønsted-acid sites, one must determine the concentration of these sites. This determination remains a nontrivial problem in zeolite catalysis. Infrared spectroscopy measurement of adsorbed pyridinium ions is one of the few techniques which is not controversial [15]; however, it is very difficult to determine the absorption coefficient needed to apply Beer's law. In addition to requiring expensive equipment, ^{27}Al NMR suffers from the problem that tetrahedral Al need not be in the zeolite framework. Measurements of the lattice parameter using X-ray diffraction [16] and of ^{29}Si NMR [17] are extremely useful for determining framework Al content in *some* zeolites; however, one should be careful in equating Brønsted-site density to framework Al content. In the important case of FAU, a majority of the charge-balancing hydroxyls are inaccessible to reactant molecules [18], so that the effective number of Brønsted sites is significantly less than the framework Al content.

3.1. TPD of ammonia

One of the most widely used methods for obtaining Brønsted-site densities is temperature-programmed desorption (TPD) of ammonia. For reasons I have discussed elsewhere [19], I do not regard this as a useful technique. Most troubling is the fact that adsorption of ammonia is not specific to Brønsted sites. Juskelis et al. showed that ammonia adsorbs more strongly on CaO than it does on a USY catalyst [20]. Since most real materials contain non-framework alumina and other species, this represents a very significant problem. In recognition of this, practitioners of ammonia TPD frequently count only those molecules which desorb above a certain temperature, sometimes holding the sample at an intermediate temperature to remove weakly held species. This approach does not alleviate the difficulties associated with TPD. First, adsorption on non-Brønsted sites may be stronger than on Brønsted sites. (While any site which adsorbs ammonia but is not a Brønsted site may be called a Lewis site, calling these Lewis sites tends to imply catalytic activity, which should not be assumed.)

Second, the temperature at which desorption occurs from both Brønsted and non-Brønsted sites depends *strongly* on conditions used for the experiment. In an example from our own work, we showed that the peak desorption temperature for ammonia from the Brønsted sites in H-MFI *shifted by more than 150 degrees for the same sample* depending on the conditions used for the measurement [1]. Finally, even qualitative analysis of ammonia TPD results should be viewed cautiously. Using a simple model of desorption which properly accounts for diffusion and readsorption in a porous material [21,22], one can show that peaks separated by 100 degrees in TPD can result from changes in the particle size of the catalyst, not necessarily different types of sites [19]. Furthermore, shifts of this magnitude can be obtained by assuming realistic and typical values for the experimental conditions and catalyst properties.

Finally, the common assumption that heats of adsorption for ammonia will correlate with reactivity is not valid, even for Brønsted sites. Calorimetric measurements comparing the H-[Fe]MFI to a normal, Al-containing sample indicated that the heats of adsorption were the same for both materials, within experimental error [23]. Yet the reactivity of Brønsted sites associated with framework substitution of Fe^{3+} is much different.

In summary, it is my opinion that ammonia is not a good probe molecule for measuring acid-site densities. Abandoning the use of ammonia TPD could clear up at least some of the confusion in this field.

3.2. TPD of amines

A technique for measuring Brønsted-site densities that we have found very useful is TPD of reactive amines [24–27]. The idea resulted from the observation that alkylammonium ions, formed by protonation of amines at Brønsted sites, react in a very narrow temperature range in TPD via a reaction similar to the Hoffman elimination reaction, as shown below:

$$\mathrm{HRNH_2 + ZOH \rightarrow HRNH_3^+ \cdots ZO^-}$$
$$\mathrm{HRNH_3^+ \cdots ZO^- \rightarrow R + NH_3 + ZOH}$$

For H-MFI samples with varying Al contents, we observed reaction of one molecule per framework Al [24,28]. Reaction of the 1 : 1 complexes was found for all amines small enough to enter the zeolite cavity, with the exception of methylamine which cannot undergo Hoffman elimination [28].

While the Brønsted-site densities that one determines do not depend on the experimental conditions, we have found it useful to perform our experiments using the apparatus which is shown schematically in figure 1. This instrument allows simultaneous thermogravimetric analysis (TGA) and TPD measurements. The TGA results are useful since one can determine whether there is a residual on the sample after desorption and one can quantify the amounts which desorb without having to calibrate the mass spectrometer. The only unique feature of this equipment is that the sample is evacuated using the same turbomolecular pump that is used for the mass spectrometer, without need for differential pumping. This ensures that the pressure above the sample is low enough to minimize secondary reactions ($\sim 10^{-5}$ Torr at the desorption peak), while allowing a high sensitivity for the mass spectrometer. In a typical TPD-TGA experiment, the sample is heated to 750 K in vacuum for removing water and other impurities and then exposed to several Torr of the amine of interest at room temperature. After evacuation, the temperature is ramped to 750 K while monitoring the sample mass and the desorbing products.

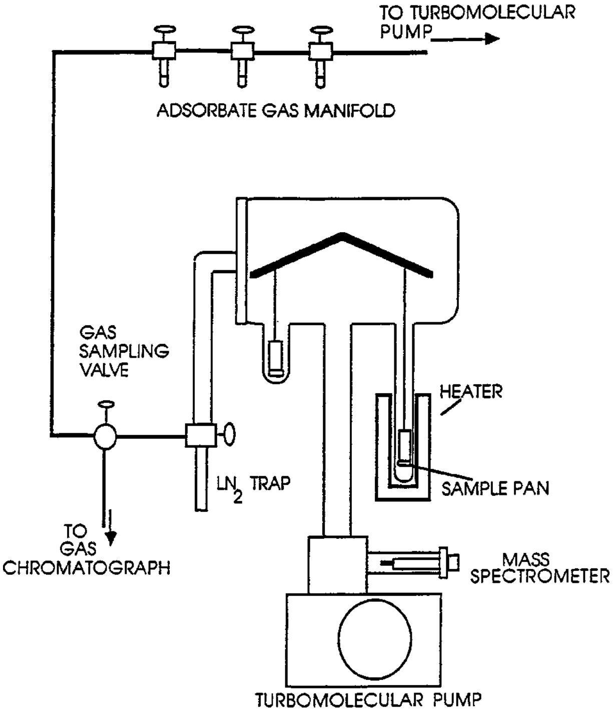

Figure 1. Diagram of equipment used in our TPD-TGA measurements. (The figure is taken from [68].)

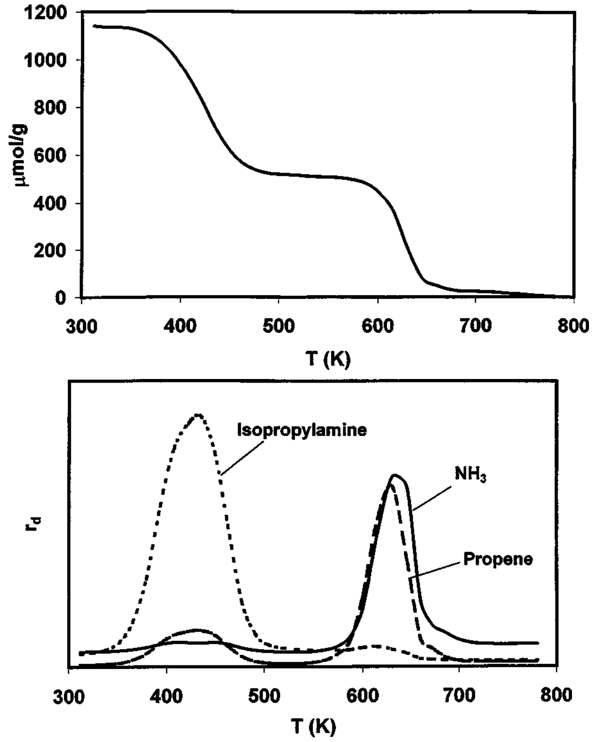

Figure 2. TPD-TGA results for isopropylamine in an H-MFI sample. The desorption of propylene and ammonia above 550 K corresponds to decomposition of the amine at the Brønsted-acid sites.

Figure 2 shows a typical result for TPD-TGA of isopropylamine from an H-MFI sample having a bulk Si/Al ratio of 26 (0.63 mmol of Al/g of sample). The initial coverage following exposure of the sample to a few Torr of vapor at 298 K and evacuation for 1 h is 1.15 mmol/g. Upon heating at 20 K/min in vacuum, unreacted amine molecules desorb below 500 K, leaving a coverage of 0.50 mmol/g. The molecules associated with low-temperature desorption can probably be assigned to a number of different types of species, including molecules associated with Lewis-acid sites, molecules associated with hydroxyl defects, and molecules which are hydrogen bonded to protonated amines at the Brønsted sites. What is more interesting is the high-

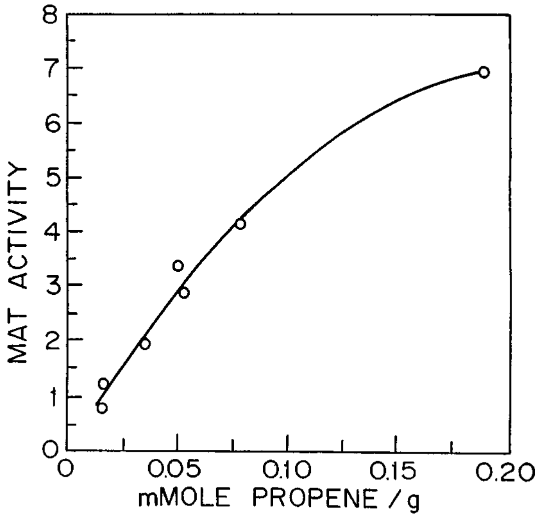

Figure 3. Relationship between MAT activities and Brønsted-site densities for a series of FCC catalysts which had been steam deactivated to varying degrees. The Brønsted-site densities were measured using TPD-TGA of isopropylamine. (The figure is taken from [30].)

temperature feature which desorbs as propylene and ammonia between 575 and 650 K. This desorption feature can be associated with protonated molecules at Brønsted sites. The concentration of Brønsted sites is frequently less than the bulk Al content, even for H-MFI, probably indicating the presence of nonframework Al. Further confirmation that the TPD-TGA results provide a true measure of the Brønsted-site density comes from the observation that the site density is independent of the choice of alkylamine, so long as the amine is small enough to fit inside the zeolite cavities [29].

That TPD-TGA results provide useful information about real catalysts is shown by the correlation with hydrocarbon cracking activity, as measured in the microactivity test (MAT) [30]. TPD-TGA measurements were performed on a series of commercial-type catalysts, which consist of 10% H-Y in a clay matrix, steam deactivated for varying lengths of time. The TPD-TGA results were similar to those shown in figure 2, with the exception that desorption of unreacted molecules extended to higher temperatures. The site density, as determined from the amount of isopropylamine which reacted to propylene and ammonia between 575 and 650 K, decreased from its initial value of 0.190 to 0.011 mmol/g after steaming for 60 h. Figure 3 shows that there is an excellent correlation of the MAT activity with the Brønsted-site density. Additional evidence that these results are significant comes from the correlation of site density with the framework Al content of the crystalline phase, shown in figure 4. For these materials, most of the Brønsted sites are present in the zeolite phase and steam deactivation is primarily due to dealumination of the zeolite.

In addition to the very practical application of correlating catalytic activities with site densities, it is also essential to know the site density before one can begin to describe the nature of acid sites in zeolites. In the next section, I will review our work on defining “acidity” in solid acids.

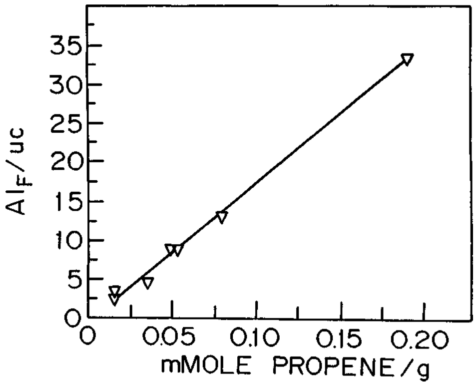

Figure 4. Relationship between the Brønsted-site density and the framework Al content of FAU phase of the same FCC samples as in figure 3. (The figure is taken from [30].)

4. Determining the nature of the acid sites

Essentially all of our work on this subject has been with high-silica zeolites like H-MFI since these materials appear to have discrete, essentially identical, non-interacting, Brønsted-acid sites [4–6]. It does not appear that the acid sites on more complex materials are dramatically different from those on H-MFI based on our adsorption studies [12,25], so that the picture that emerges from examining H-MFI should be applicable to other zeolites as well.

4.1. Stoichiometric adsorption complexes

To truly describe any surface-catalyzed reaction, one needs to know the stability and chemical structure of reactants, products, and intermediates at the catalytic sites. Therefore, the observation that one forms stoichiometric adsorption complexes, one per Brønsted site, for many types of molecules, is extremely important. Such 1 : 1 complexes have been identified in H-MFI for alcohols [31–33], amines [28], nitriles [34], pyridines [35], thiols [36], ketones [37,38], CO [39], diethyl ether [34], and, most recently, metal halides [40,41].

The clearest method to observe the 1 : 1 complexes comes from TPD-TGA results, such as those described for isopropylamine in section 3. However, adsorption complexes can also be identified using microcalorimetry and NMR spectroscopy. In figure 5, differential heats are shown for pyridine on three H-MFI samples with different Si/Al ratios, using a home-built instrument which has been described elsewhere [42,43]. These measurements were performed at 480 K, a crucial point since TPD-TGA studies of pyridine demonstrate that it will not be possible to ensure equilibrium will be reached at lower temperatures [44]. Figure 5 shows that the differential heats are 200 kJ/mol up to the coverage of one per site, independent of Si/Al ratio. For coverages above 1 : 1, the heats fall rapidly to

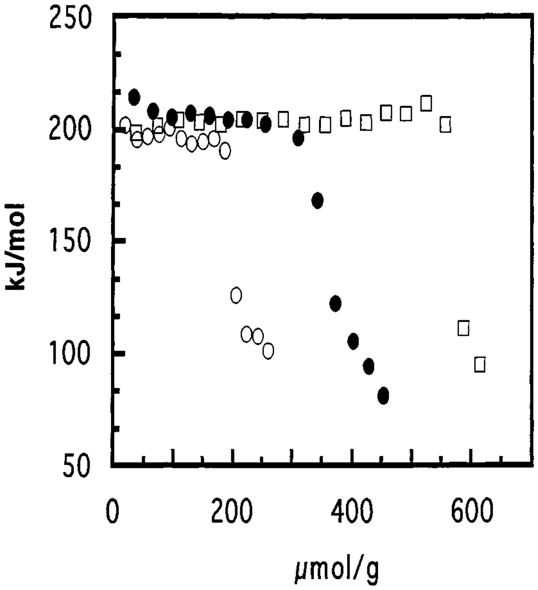

Figure 5. Differential heats of adsorption for pyridine on three H-MFI samples with varying Al contents. The drop in the heats occurs at the Brønsted-site density for each sample. (The figure is taken from [43].)

a value of 70 kJ/mol [45], a value which is reasonable for adsorption of pyridine on the siliceous walls of the MFI cavity.

It is important to recognize that the data in figure 5 do not prove that the sites in H-MFI are energetically equivalent [44]. TPD-TGA measurements carried out in vacuum for pyridine on H-MFI indicate that those molecules associated with the 1 : 1 complex are immobile below 600 K [44]. Therefore, one should expect that the molecules will stick to the first site they encounter; they will not be able to sample all sites in the zeolite, so as to find the energetically preferred sites. The data in figure 5 are obviously consistent with all of the sites being equivalent and the differential heats in the 1 : 1 region must be the average heat of formation of the 1 : 1 adsorption complex.

^{13}C NMR spectra of acetonitrile ($CH_3{}^{13}CN$) and acetone ($CH_3{}^{13}COCH_3$) provide additional evidence for 1 : 1 complexes and again suggest equivalence of the Brønsted sites [37,38,46]. For both adsorbates, the ^{13}C NMR lineshapes at 298 K show a partially narrowed, axially symmetric, chemical-shift tensor at loadings below one per Brønsted site. At higher loadings, the linewidth decreases dramatically due to molecular reorientation at the acid sites and exchange with physically adsorbed molecules, giving rise to a Lorentzian lineshape at a frequency corresponding to the isotropic chemical shift. The transition from one coverage regime to the other is shown in figure 6 for acetonitrile, where the linewidth at half maximum is plotted as a function of fractional surface coverage, calculated using the Brønsted-site density from TPD-TGA of isopropylamine [46]. Similar results were obtained for acetone [37]. For loadings below the 1 : 1 value, neither the lineshape nor the isotropic shift change with temperature. Furthermore, within experimental error, all

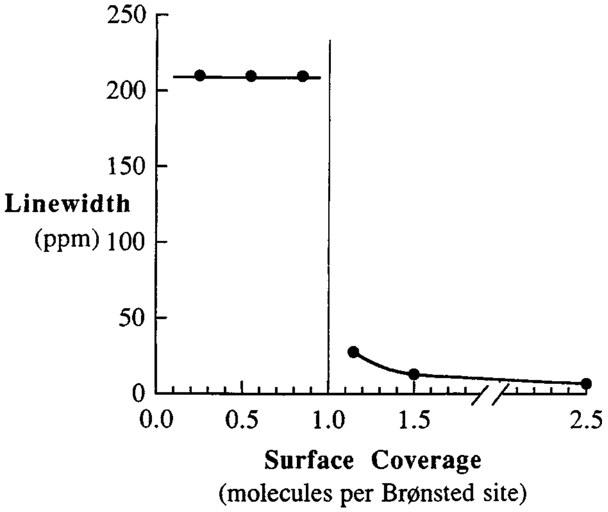

Figure 6. Proton-decoupled ^{13}C NMR lineshapes of acetonitrile adsorbed on H-MFI as a function of coverage. The linewidths (●) are of the tensor for concentrations below one molecule/site and FWHM of the Lorentzian at higher loadings. (The figure is taken from [69].)

species hydrogen bonded to Brønsted-acid sites are identical [38,47].

4.2. Calorimetric measurements

We have viewed calorimetric measurements of stoichiometric adsorption complexes as a powerful method for defining solid acidity by comparing thermodynamic properties in zeolites to thermodynamic properties in homogeneous acids [1]. While acidities in homogeneous media are usually defined by an equilibrium constant, any equilibrium constant can be related to the change in free energy of the reaction ($K = \exp\{-\Delta G/RT\}$) and the change in free energy can be related to the change in enthalpy and entropy of reaction ($\Delta G = \Delta H - T\Delta S$). In the case of the solution-phase acids, the free energy is $\Delta G_{\mathrm{prot,sol}}$ and the reaction in question is the following:

$$H^+_{(\mathrm{sol})} + B_{(\mathrm{sol})} \rightleftharpoons HB^+_{(\mathrm{sol})}$$

If the solvent is water, $H^+_{(\mathrm{sol})}$ is the aqueous hydronium ion and $-\log K$ is defined as $\mathrm{p}K_a$. It is important to recognize that the energies associated with placing both B and HB^+ in the solvent are comparable to the energy of the protonation reaction itself, so that solvation effects can be very large [1]. Equilibrium constants can also be measured in the gas phase, and the gas-phase measurements provide an intrinsic measure of acidity since there are no solvent effects. Usually, equilibrium constants in the gas phase are reported in terms of the gas-phase basicity (GB $= -\Delta G$) or the gas-phase proton affinity (PA $= -\Delta H$). For both the gas phase and solution phase, ΔH can be determined unambiguously from the temperature dependence of the equilibrium constant, although ΔS is sometimes essentially constant for a series of similar reactions [48].

Considering only pyridine, it is immediately apparent that $-\Delta H$ for the protonation reaction in H-MFI is much larger than it is in aqueous solutions. Taking $-\Delta H_{\text{pro,zeo}}$ to be the difference between the heat of adsorption on the Brønsted sites (200 kJ/mol) and the heat of adsorption at coverages above one per site (70 kJ/mol), one calculates the enthalpy change for the proton-transfer reaction to be 130 kJ/mol in the zeolite. By comparison, $-\Delta H_{\text{pro,aqu}}$ is approximately 20 kJ/mol. This difference will have a tremendous impact on reaction kinetics. For example, the activation energy for the deprotonation reaction must be at least as large as $-\Delta H_{\text{pro,zeo}}$ in the absence of a simultaneous displacement by another species [49].

It has been suggested that solvent effects in the zeolite can be induced, and the barrier for deprotonation lowered, through the presence of coadsorbed species; however, in a study of the effect of n-hexane coadsorption with pyridine, we showed that the effect of the coadsorbed "solvent" was minimal [50]. While coadsorption of polar molecules may produce larger effects, it is not obvious that coadsorbed molecules in zeolite micropores are similar to a bulk solvent. Clearly, one should not expect to run reactions in zeolites under the same conditions used in solution phase, even if the zeolite is placed in the liquid phase.

An interesting method for comparing homogeneous and solid acids is to compare the enthalpies of protonation for a series of molecules. This comparison has been made for a series of amines, ring-substituted pyridines, nitriles, and alcohols [34,35,51]. In figure 7, I have plotted the differential heats for the 1 : 1 adsorption complexes for various amines, pyridines, and acetonitrile in H-MFI as a function of the heat of protonation in aqueous solution. I have excluded alcohols from this figure because of their tendency to form hydrogen-bond networks in the zeolite, making the heat of formation of the 1 : 1 complexes somewhat complicated [34]. I have also not attempted to subtract off the van der Waals component of the differential heats, but these values are likely to be relatively small and similar for most of the molecules examined. Figure 7 shows that there is a very poor correlation between heats of protonation in the zeolite and heats of protonation in the aqueous phase. The difference between the amines and pyridines is particularly striking, but easy to understand. Amines and their ammonium ions tend to form strong hydrogen bonds with water and are solvated to a very different extent than are pyridine and pyridinium ions.

An immediate implication of the poor correlation in figure 7 is that attempts to define acidity in the zeolite in terms of an effective pK_a or Hammett acidity (H_0) are completely inappropriate. This solution-phase approach assumes that interactions of the acid sites with reactant bases will scale in a regular manner to that found for acids in aqueous solutions, a result which is not even qualitatively true. Therefore, it should not be surprising that *radically* different values for acidity are often reported in the literature, depending on whether the probe bases are Hammett indicators like nitrotoluene or ketones like mesityl oxide or acetone [52]. Similar problems occur when one tries to use a solution-phase approach to predict energy barriers and reaction coordinates for typical reactions.

The correlation between the differential heats in H-MFI and gas-phase proton affinities is much better, as shown in figure 8. Figure 8 includes data for the same molecules as in figure 7, as well as a series of nitriles, since proton affinities for these are readily available [48]. The line on the plot is not a best fit to the data, but rather was drawn to intersect the point for ammonia ($-\Delta H_{\text{pro,zeo}} = 145$ kJ/mol, PA $=$ 858 kJ/mol) with a slope of one. The correlation between differential heats and proton affinities is remarkable. More important, however, is the fact that this comparison allows

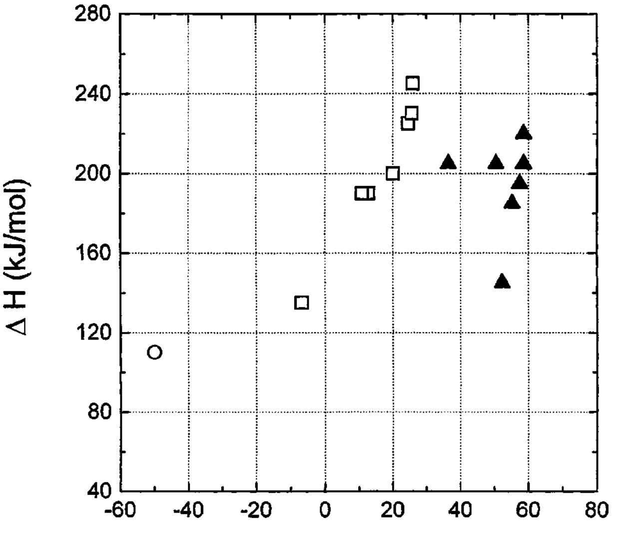

Figure 7. Plot of the heat of formation of the 1 : 1 complex in H-MFI versus the enthalpy of protonation in aqueous solutions: (□) pyridines, (▲) amines, and (○) acetonitrile.

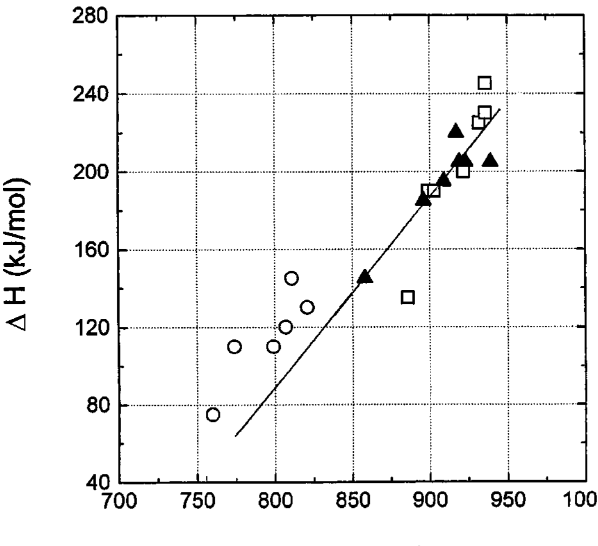

Figure 8. Plot of the heat of formation of the 1 : 1 complex in H-MFI versus the gas-phase proton affinities: (□) pyridines, (▲) amines, and (○) nitriles. The line in the figure was drawn to intersect the point for ammonia and have a slope of one.

one to determine which effects are important in stabilizing the adsorption complex and estimate the magnitude of these effects.

The following, hypothetical, thermochemical cycle is helpful for understanding bonding at the Brønsted sites:

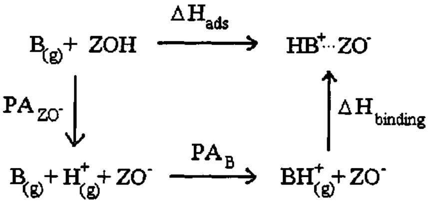

In this scheme, the heat of formation of the 1 : 1 adsorption complex is split into three steps, including removal of the proton from the zeolite into the gas phase, reaction of the gas-phase base with the proton, and finally reaction of the gas-phase ion with the framework anion. A straight-line, slope-of-one correlation between the differential heats and the gas-phase, proton affinities implies that the sum of $\mathrm{PA}_{\mathrm{ZO}}$- and $\Delta H_{\mathrm{binding}}$ is constant, which in turn implies that $\Delta H_{\mathrm{binding}}$ is constant. Using a value of 1300 kJ/mol for $\mathrm{PA}_{\mathrm{ZO}}$-, one can estimate $\Delta H_{\mathrm{binding}}$ for the line in figure 8 to be approximately 590 kJ/mol, which is very reasonable for bringing two oppositely charged particles together from infinity to the known bond distance [1].

For the amines and pyridines, the assumption of proton transfer is valid, and the deviations of data points from the line in figure 8 provide insights into the nature of the zeolite–adsorbate bond. This has been discussed in detail elsewhere [35,51]. For this discussion, it is worth pointing out that it is usually easy to rationalize the cause for deviation from the correlation. For the nitriles, the 1 : 1 adsorption complexes are formed through hydrogen bonds with the Brønsted sites and proton transfer is incomplete. Even in this case, it is known that hydrogen-bond strengths correlate with proton affinities [53], a trend which is followed in the zeolite. Furthermore, it is tempting to speculate that the protonated forms of the nitriles, if they exist as stable species, may lie on the line in figure 8, but that the hydrogen-bonded species, being more stable, lie above the line.

The intent of this discussion was to demonstrate that calorimetry provides a powerful framework for understanding acidity in zeolites. It should be possible to extend these concepts to reaction chemistry using methodologies that will be discussed later in this paper.

4.3. NMR measurements

In recent years, there has been a great deal of interest in using NMR to characterize and describe zeolite acidity, including work by our group [38,47]. In particular, attempts have been made to use the isotropic, ^{13}C chemical shift for ketones as a measure of acidity based on correlations developed in solution-phase acids. However, while NMR provides a great deal of information on the nature of the adsorption complex, there are issues which need to be addressed in the interpretation. For starters, solution-phase comparisons are inappropriate and no single set of probe molecules will provide an accurate overall picture of acidity in the solid, as I have already discussed in detail. Furthermore, it is crucial that one examines adsorption under known conditions, with loadings at or below one per Brønsted-acid site, since serious errors are introduced at higher loadings.

One must also recognize that the isotropic shifts for ketones depend strongly on the environment the molecule finds itself in. For example, it is tempting to infer something about the hydrogen-bond strength for the 1 : 1 complex of acetone ($\mathrm{CH_3{}^{13}COCH_3}$) in H-MFI from the observation that the ^{13}C isotropic shift is 205 ppm in the pure liquid (relative to TMS), 244 ppm in concentrated sulfuric acid, and 223 ppm in the 1 : 1 complex. The problem is that large isotropic shifts are observed for phase changes (the shift for gas-phase acetone is 198 ppm, while it is 209 ppm for the solid) and for van der Waals interactions (the isotropic shift on silicalite is 215 ppm) [38]. Furthermore, one observes large chemical shifts on Lewis acids, like alumina (233 ppm), which should clearly not be associated with super acids [52]. Therefore, the isotropic chemical shifts probably do *not* provide a simple measure of acid strength.

Together with infrared spectroscopy, NMR is an extremely powerful technique for determining the structure of stable adsorption complexes. Along with many other groups, we have used NMR to examine species formed by adsorption and reaction at the acid sites [47,54]. However, as with the results from any technique, the data is most powerful when used in combination with other techniques, such as determination of adsorption stoichiometry and identification of end products from TPD [55]. Over-interpretation of isotropic shifts, without corroborating spectroscopic information, can lead to incorrect assignments. An example of this is the recent report of large, reversible changes in the ^{13}C isotropic shifts as a function of temperature for the adsorption complex formed acetonitrile ($\mathrm{CH_3{}^{13}CN}$) in H-MFI [56]. The isotropic shift is 115 ppm at 78 K, but shifts to 133 ppm at 450 K [57]. A change this large would normally be associated with a rapid equilibrium between two species, say a nitrile (115 ppm) and an imine ($\sim$180 ppm). IR measurements performed using the same experimental conditions, however, provide no evidence for a reversible change in bond order of the adsorption complex [57]. Preliminary calculations suggest that vibrational excitation of low-frequency bending modes of the complex can lead to large changes in the isotropic shift and that these may be responsible for the temperature effects [58]. Similarly, ambiguities in the interpretation of ^{13}C NMR spectra obtained for intermediates formed by adsorption of allyl alcohol in H-MFI could only be resolved using other techniques, since NMR could not discriminate between hydrogen-bonded propanal and a stable allyl cation [55].

5. Reaction chemistry

Descriptions of acidity are only useful if they can be used to understand or predict catalytic chemistry. Typical definitions, such as Hammett acidities or effective $\mathrm{p}K_\mathrm{a}$'s, would not be useful, even if they were appropriate, since they do not allow one to predict reaction chemistry. To describe a surface-catalyzed reaction, a better approach is to determine structures and energies of all species along a given reaction coordinate. The concepts described in the previous section attempt to fulfill that requirement.

The importance of recognizing that stoichiometric adsorption complexes are formed at Brønsted sites should not be minimized. The fact that one has a discrete number of essentially identical sites in zeolites like H-MFI is essential for examining and predicting reaction chemistry. Studying the structure and measuring the energies of these complexes provides a true starting point for the understanding of acid–base chemistry. The correlation between the differential heats of adsorption at loadings below one per site (essentially, the heat of formation of the adsorption complex) and gas-phase proton affinities is also very helpful. Finally, spectroscopic measurements determine what structures are formed for the adsorption complex.

5.1. Alcohol dehydration reaction

The practical application of the concepts developed in section 4 is best demonstrated by example, considering the simple dehydration of adsorption complexes formed by simple alcohols in H-MFI. It is reasonable to hypothesize that the most important species along the reaction coordinate would be as follows:

$$\begin{aligned}&\mathrm{HROH} + \mathrm{ZOH} \rightleftharpoons \mathrm{HROH_2^+} \cdots \mathrm{ZO^-} \rightleftharpoons\\&\quad \mathrm{H_2O} + \mathrm{HR^+} \cdots \mathrm{ZO^-} \rightleftharpoons \mathrm{H_2O} + \mathrm{R} + \mathrm{ZOH}\end{aligned}$$

Here, the assumption is that the 1 : 1 complex formed by adsorption of the alcohol (HROH) from the gas phase is a zeolite-bound oxonium ion ($\mathrm{HROH_2^+} \cdots \mathrm{ZO^-}$). Dehydration occurs through formation of water and a zeolite-bound carbenium ion ($\mathrm{HR^+} \cdots \mathrm{ZO^-}$), which in turn loses a proton to desorb as the olefin (R). If one next makes the assumption that heats of formation of the adsorption complexes can be determined from the straight-line correlation in figure 8, the energies of each species in the reaction scheme can be calculated from tabulated proton affinities. (In the absence of data, gas-phase proton affinities can also be calculated with good accuracy [55].) For alcohol dehydration, the calculated energies are shown in figure 9 [33]. All energies are referenced to the gas-phase alcohols, and standard heats of reaction were used to calculate the energies of the olefin and water products. Tabulated proton affinities of the alcohols and olefins were used to determine the difference in the energy of adsorption complexes from the gas-phase species, using the line in figure 8.

Figure 9 allows a number of interesting predictions about the alcohol dehydration reactions in H-MFI. Based on these results, one would expect that each of the gas-phase alcohols should adsorb onto the Brønsted sites and form stable, oxonium-ion, adsorption complexes, with only modest energy differences between the various alcohols. The overall heats of reaction to olefin products are also similar for the various alcohols. However, if one assumes that the activation barrier for dehydration is equal to the energy difference between the oxonium-ion and carbenium-ion complexes, one predicts that there should be dramatic differences in the reaction chemistries. In the case of methanol, formation of the methyl carbenium ion is extremely unfavorable, requiring more than 55 kcal/mol (230 kJ/mol) starting from the oxonium ion. By contrast, the energy difference between the oxonium and carbenium ions for t-butanol is only 8 kcal/mol. A barrier of this size is small enough so that one would expect relatively fast reaction rates, even at room temperature, based on transition-state theory.

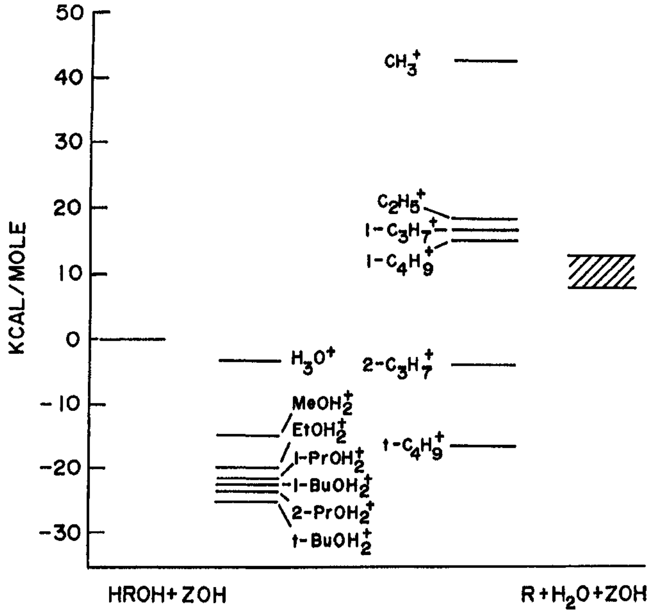

Figure 9. Potential energy diagram of alcohol/H-MFI interactions. The adsorption of alcohols and olefins on the zeolite is assumed to occur through proton transfer, allowing the use of known proton affinities to calculate relative heats of formation. (The figure is taken from [33].)

The predictions for alcohol dehydration agree remarkably well with observations from adsorption studies [33]. Starting from the 1 : 1, alcohol adsorption complexes, one observes that methanol and ethanol desorb intact in TPD-TGA studies carried out in vacuum. The 1 : 1 complex for isopropanol, which decomposes via a secondary cation, reacts to propene and water at ∼400 K. Finally, *tert*-butyl alcohol reacts at room temperature; water can be removed from the sample by evacuation, leaving a *tert*-butyl complex.

Starting from the gas-phase olefins on the right side of figure 9, one also predicts significantly different reactivities for olefins that form primary, secondary, or tertiary carbenium ions. Formation of secondary and tertiary carbenium ions is predicted to be energetically favorable compared to the gas-phase olefins, while formation of primary carbenium ions is not. This prediction matches experimental observations well in the case of ethylene, propylene, and isobutylene [10]. Propylene reacts rapidly to oligomers in H-MFI at room temperature, stopping only after the region surrounding the Brønsted sites is filled by the oligomers. In the case of isobutylene, the TPD results for *tert*-butyl alcohol showed that the isobutylene formed by dehydration was so reactive that only oligomerization and cracking products were observed. In both cases, the reaction almost certainly proceeds by reaction of a gas-phase olefin with an adsorbed carbenium ion; and the observations demonstrate that secondary and tertiary carbenium ions must be very stable. By contrast, ethene is relatively unreactive at room temperature, with rapid formation of oligomers only after heating the sample above ~370 K. This low reactivity is to be expected based on the low stability of primary carbenium ions.

5.2. Carbenium ion formation

Obviously, the model upon which figure 9 is based is overly simplistic. Most important, the thermochemistry, predicted from the linear correlation in figure 8, assumes that all adsorption complexes exist as zwitterion complexes, with complete proton transfer from the zeolite framework. In the case of alcohols, calculations suggest that the stable complex is actually a hydrogen-bonded species, although the energy difference between the hydrogen-bonded complex and the oxonium ion appears to be only a few kJ/mol in the case of methanol [59]. More surprising, the model predicts that isopropyl and *tert*-butyl carbenium ions are stable with respect to the gas-phase olefins. The question is whether or not this can be verified experimentally.

Most attempts to study carbenium ions spectroscopically start by forming the intermediates by simple adsorption of olefins. However, direct adsorption of olefins results in a very complex adsorption system due to rapid oligomerization [60]. For example, propylene reacts so rapidly to oligomers in H-MFI at room temperature that even our attempts to titrate a small fraction of the sites at low pressures led to oligomers at those sites which were filled [10]. Because a complex mixture of adsorbed species are formed under these conditions, spectroscopic measurements are ambiguous.

Adsorption of *tert*-butyl alcohol provides a simpler method for identifying the nature of the *tert*-butyl complex. Figure 10 shows the TPD-TGA curves after adsorption of *tert*-butyl alcohol in H-MFI at room temperature, followed by 1 h evacuation [33]. In this figure, the TGA results are reported as molecules per Brønsted site, with zero given as the initial weight of the sample before adsorption. Starting from a coverage of one molecule per site, only olefin products ($m/e = 41$) and a small amount of water ($m/e = 18$) are observed leaving the sample. The amount of water which desorbs is significantly less than one molecule per site, so that most of the water formed by dehydration of the alcohol must have left the sample during the evacuation.

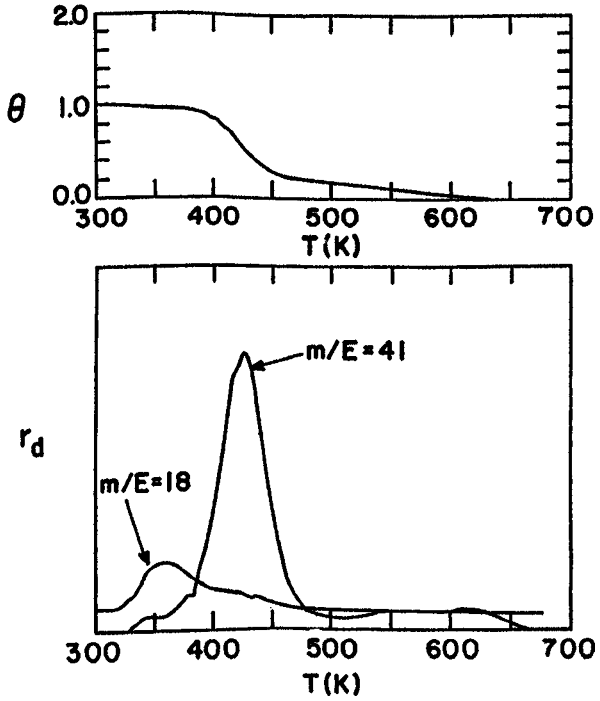

Figure 10. TPD-TGA curves following adsorption of *tert*-butyl alcohol on H-MFI. Most of the water formed by dehydration desorbs during evacuation, prior to performing the TPD-TGA experiment. All desorbing olefins were monitored using $m/e = 41$; however, the peak centered at 430 K includes a wide mixture of olefin products. (The figure was taken from [33].)

Furthermore, GC analysis of the olefin products indicates that this is not primarily isobutylene [10]. Rather, a mixture of products (ranging from ethene to C_7 olefins, in the same ratios found for TPD of propylene oligomers [10]) are formed, indicating that oligomerization and cracking occur prior to desorption. These data suggest that one can form the 1 : 1, *tert*-butyl, stoichiometric adsorption complex in H-MFI by this method.

While the *tert*-butyl adsorption complex has the stoichiometry of a *tert*-butyl carbenium ion, ^{13}C NMR results for adsorption of $(CH_3)_3{}^{13}COH$ in H-MFI indicate that the structure is that of an alkoxide, or a silyl ether [61], as shown below:

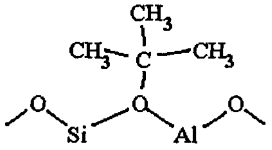

It is easy to rationalize why this must be the case. In super acids, where stable *tert*-butyl carbenium ions are the stable species, the anion must be non-nucleophilic and one must have a high dielectric solvent to reduce the energy associated with separating the cation from the anion. While the zeolite, framework anion may well be non-nucleophilic, there is no dielectric solvent to lower the energy of charge separation.

However, at least for the *tert*-butyl species, this intermediate must be very close in energy to the carbenium ion,

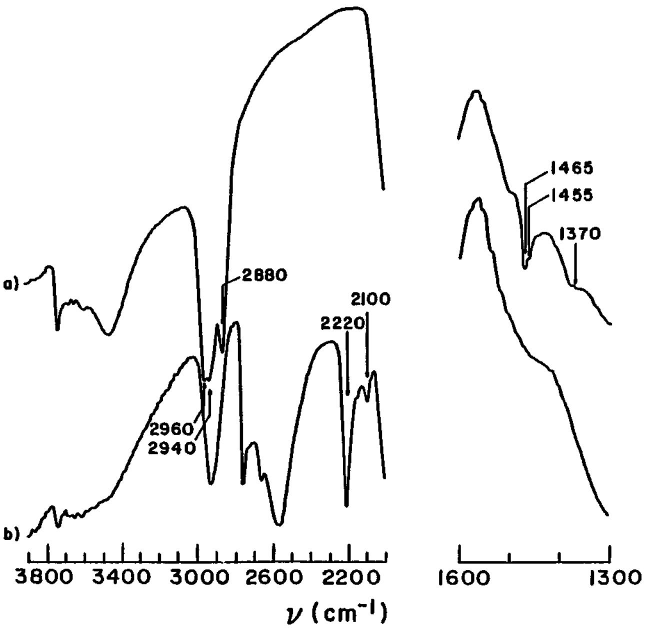

Figure 11. *Tert*-butyl alcohol adsorbed on H-MFI before (a) and after (b) exposure to D_2O at 295 K. (The figure is taken from [62].)

as demonstrated by other observations. First, there is the high reactivity of this species evident from the TPD results. Second, IR spectra of *tert*-butyl group formed by alcohol adsorption in H-MFI under conditions similar to those used in the TPD-TGA studies indicate that the C–H bonds are labile at room temperature. Figure 11 shows the spectra obtained following adsorption and evacuation of *tert*-butyl alcohol in H-MFI [62]. Spectrum (a) shows a broad band for the ν(C–H) stretches between 2800 and 3000 cm^{-1}. While oligomerization may occur to a limited extent during evacuation, the fact that the Brønsted sites associated with the hydroxyl stretch at 3605 cm^{-1} are not observed in the spectrum at a coverage of one molecule per site implies that the *tert*-butyl intermediates remain at the acid sites. Spectrum (b) shows the changes that occur when the sample in (a) is exposed to a few Torr of D_2O and then evacuated. In addition to exchange of the hydroxyl bands for their deuterium analogs, a strong band between 2100 and 2220 cm^{-1} is observed in the spectrum, indicating formation of C–D bonds. While the mechanism for H–D exchange into the alkyl group is uncertain, this exchange almost certainly indicates rapid, even if transient, formation of carbenium ions.

The spectroscopic and reactivity data for *tert*-butyl alcohol adsorption in H-MFI have been used to estimate the barrier between the *tert*-butyl alkoxide intermediate and the *tert*-butyl carbenium ion [61]. For this discussion, the main point is that the *tert*-butyl intermediate must be very close in energy to a carbenium ion and may probably be considered a carbenium ion for mechanistic purposes. For other intermediates, the most important question is how to determine the energy barriers between adsorbates and the reactive intermediates or transition states. Because the energy of the alkoxide bond should not be a strong function of the alkyl group, while the carbenium ion stability will depend very strongly on whether the cation is primary, secondary, or tertiary, this energy difference will depend strongly on the alkyl group.

6. H-[Fe]MFI: an opportunity and an enigma

In our experience, the sites generated by framework substitution of Al in siliceous zeolites are very similar, independent of zeolite structure [25]. The nature of adsorbed species and the chemistry these species undergo are found to be essentially the same for high-silica zeolites. However, the sites generated by framework substitution of Fe^{3+} are quite different. Results on these materials suggest that they may be useful for performing selective, catalytic chemistry. The results also indicate that some of our assumptions about the relationship between catalytic properties and the adsorption properties of our most common probe molecules are not valid.

First, framework substitution of Fe into the siliceous, MFI framework generates a Brønsted site which is capable of catalyzing reactions. If care is used in the synthesis and activation of H-[Fe]MFI, TPD-TGA measurements with isopropylamine indicate that there is one Brønsted site per Fe, as demonstrated by the formation of propylene and ammonia between 575 and 650 K [26]. Stoichiometric, $1:1$ adsorption complexes, one molecule per Fe, are also observed for simple alcohols [26], acetonitrile [63], and acetone. However, the sites generated by framework Fe are clearly different. The cracking rates for n-hexane are negligible at conditions where significant rates are observed on framework Al sites [23]. Furthermore, oligomerization rates for propylene are negligible at temperatures up to at least 400 K [63]. In TPD-TGA of *tert*-butyl alcohol, isobutylene desorbs intact on H-[Fe]MFI, whereas oligomerization and cracking dominate the process on H-[Al]MFI [63]. It seems likely that either carbenium ions or the alkoxide species must be destabilized at Fe sites relative to Al sites.

Whatever the reason for the differences between H-[Fe]MFI and H-[Al]MFI, the results are exciting because they suggest that it may be possible to perform selective chemistry on the ferrosilicate. A major problem in the application of zeolites for performing selective chemistry is that olefins are so reactive that the processes are difficult to control. It is probably not possible to avoid oligomerization in normal, Al-containing zeolites and the intentional formation of small olefin products rather than gasoline is a sensitive function of the process conditions. In the case of H-[Fe]MFI, it should be easy to avoid oligomerization for reactions involving olefins. How these materials may be used effectively requires additional investigation.

The enigma comes from the fact that our most common probes of acid strength do not distinguish between framework Fe and Al sites [23,63]. Figure 12 shows the differential heats for pyridine on H-[Fe]MFI, H-[Ga]MFI,

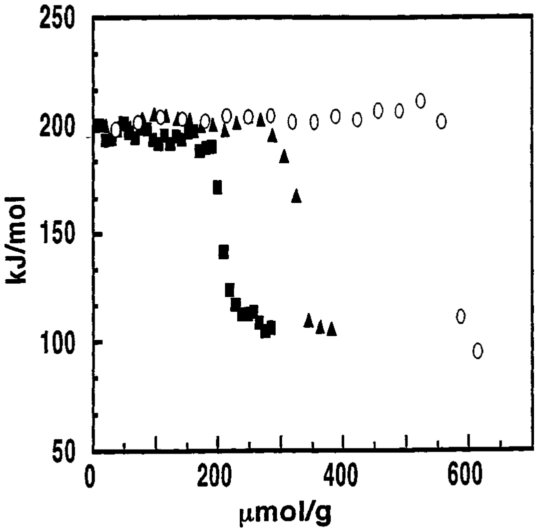

Figure 12. The differential heats of adsorption for pyridine in H-[Fe]MFI (■), H-[Ga]MFI (▲), and H-[Al]MFI (○). (The figure is taken from [23].)

and H-[Al]MFI. While the site density of the H-[Fe]MFI sample is significantly less in this example, due to the low Fe content, the differential heats on each of the samples in the 1 : 1 coverage regime are 200 kJ/mol, within experimental error. The conclusions from ammonia adsorption, where the heats of formation of the 1 : 1 complexes are 145 kJ/mol, are the same [23]. One could argue that ammonia and pyridine are not good probe molecules because proton transfer is complete following adsorption, while most reactant molecules are hydrogen bonded to the site. However, characterization of the acid sites with acetonitrile resulted in the same ν(C–N) stretching frequency, 2298 cm^{-1}, for Brønsted sites associated with both framework Fe and Al [63]. The heats of formation of the 1 : 1 complexes were also similar.

While one can generate site densities on solid acids with the appropriate choice of probe molecule, it is clear that screening for "acidity" with a single probe molecule is not appropriate, whether the probe molecule is pyridine, ammonia, acetonitrile, or anything else. In the case of H-[Fe]MFI, the use of any of the above probe molecules would lead to the conclusion that the Brønsted sites are very similar to those formed by framework Al. A better approach to characterizing the chemistry on the sites involves examining the adsorption of reactant and product molecules for the reaction of interest. This approach is clearly not as simple, but will provide a much more reliable picture of what can be expected under catalytic reaction conditions.

7. Effect of pore geometry on reactions

The catalytic activity and selectivity are affected by the environment surrounding the site. This environment is largely the result of van der Waals attractions and repulsions with the zeolite cavity in the immediate vicinity of the site. Even for cases where diffusion does not limit reaction, one should expect reactions to change with framework structure. It is convenient to consider two aspects of structural effects, concentration differences due to sorption and confinement of the reactant molecule at the site, separately.

7.1. Sorption effects

A significant number of papers have pointed out the importance of "sorption" effects on reaction rates [6,64]. For example, in the case of paraffin cracking, it is common for the rate to be expressed in terms of the pressure of the paraffin (P),

$$r = k_{\mathrm{app}}P.$$

However, the rate should more properly be written in terms of the paraffin coverage (θ),

$$r = k_{\mathrm{int}}\theta.$$

If adsorption is described by Henry's law, with a proportionality constant K, the apparent rate constant, k_{app}, will be the product of k_{int} and K. While the interaction between simple paraffins and the acid sites will be weak, so that molecules will not adsorb preferentially on the Brønsted sites, the siliceous cavity of the zeolite structure will concentrate the molecules in the cavity and, therefore, in the vicinity of the acid sites.

Since K depends exponentially on the heat of adsorption of the paraffin, it is interesting to consider how strongly pore structure affects the heat of adsorption. In figure 13, differential heats are plotted for ethane in three, one-dimensional, siliceous zeolites with different pore radii [65]. Results are shown for TON (a 10-membered-ring zeolite with pore diameter of ~0.50 nm), MTW (a 12-membered-ring zeolite, ~0.57 nm), and UTD-1 (a 14-membered-ring zeolite, >0.70 nm). While a detailed discussion of this data is given elsewhere [65], it is important to realize that the heats of adsorption and the isotherm are strongly affected by the pore size. For ethane, the interaction with the cavity decreases sharply with increasing pore diameter, going from ~38 kJ/mol on TON to 23 kJ/mol on UTD-1 at low coverages. As discussed above, the decrease in the heat of adsorption will be reflected as an increase in the apparent activation energy and a decrease in the reaction rates, even if the acid sites are otherwise identical.

7.2. Confinement of reactants and products

The sorption effects described in section 7.1 are not specific to the region surrounding the acid site and do not provide a microscopic picture of how the cavity interacts with adsorbed molecules. We have recently demonstrated that NMR is a powerful method to characterize the confinement of reactant molecules due to cavity interactions on the molecule bound to the Brønsted sites [46,66]. A key finding which provides a basis for these studies is the data shown in figure 6, which demonstrates that acetonitrile molecules are localized at the Brønsted sites when the adsorbate loading is less than one per site. Similar findings were found for acetone [37].

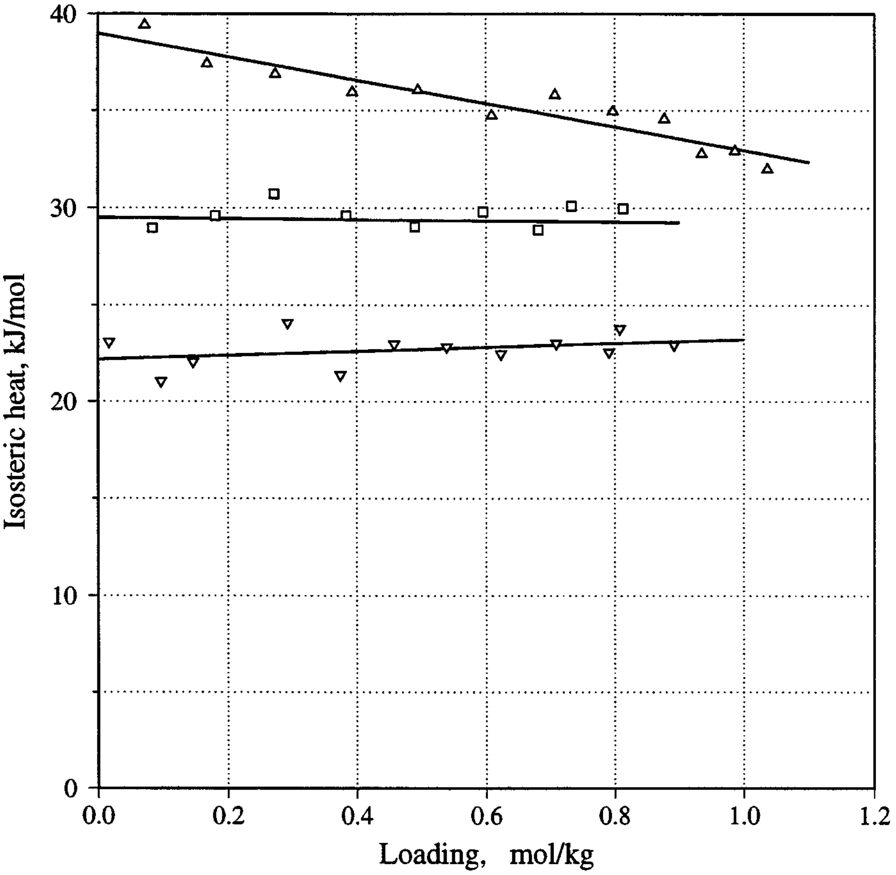

Figure 13. Isosteric heats of adsorption of ethane on siliceous materials with one-dimensional channels at 298 K: (△) TON, (□) MTW, and (▽) UTD-1. (The figure is taken from [65].)

Our work on the confining effect of the cavity on acetone and acetonitrile is reviewed elsewhere and I will not repeat the discussion here [67]. In essence, we find that static ^{13}C NMR spectra for acetone ($CH_3{}^{13}COCH_3$) and the ^{1}H NMR spectra for CH_3CN on a deuterated zeolite are partially motionally averaged at room temperature [37,52]. Of special significance, the extent of motional narrowing depends on the size of the zeolite cavity, so that dynamical studies of these molecules using NMR spectroscopy can probe the molecule–cavity interactions [46,66]. We believe these results have exciting possibilities for understanding shape selectivity in zeolite catalysts.

8. Conclusions

(1) Brønsted site densities can be easily measured using TPD studies of alkylamines which can undergo Hoffman elimination. However, ammonia is not a good probe of acidity because adsorption is not specific to the Brønsted sites.

(2) In defining site strengths, we should avoid using solution-phase terminologies. Heats of adsorption for simple bases scale much better with gas-phase proton affinities and these concepts provide a reasonable basis for predicting the reaction chemistry of simple molecules.

(3) ^{13}C NMR isotropic shifts of simple probe molecules, such as ketones and nitriles, do *not* provide a meaningful measure of acid strength.

(4) Studies of H-[Fe]MFI suggest that it may be possible to carry out reactions selectively in the presence of olefins. However, common probes of acidity in H-[Fe]MFI give similar results to that found on H-[Al]MFI, even though the catalytic activities are very different, calling into question many assumptions about how we typically characterize solid acids.

(5) Physical interactions between an adsorbed molecule and the region surrounding the site can have a significant effect on reactions. Dynamical studies using ^{13}C and ^{1}H NMR of molecules associated with 1 : 1 adsorption complexes provide an exciting new way to probe these molecule–cavity interactions.

Acknowledgement

I am grateful to the National Science Foundation for its long-term support of this work. Many of the ideas presented here resulted from a close collaboration with

Dr. W.E. Farneth (DuPont) and Professor David White (Penn Chemistry). The work would not have been possible without the assistance of Dr. George Kokotailo, who taught us how to make zeolites. Finally, I am grateful to the many excellent students who actually performed the work described in this paper.

References

[1] W.E. Farneth and R.J. Gorte, Chem. Rev. 95 (1995) 615.
[2] R.J. Gorte and D. White, Topics Catal. 4 (1997) 57.
[3] P.B. Venuto, Micropor. Mater. 2 (1994) 297.
[4] D.H. Olson, W.O. Haag and R.M. Lago, J. Catal. 61 (1980) 390.
[5] W.O. Haag and N.Y. Chen, in: *Catalyst Design: Progress and Perspectives*, ed. L.L. Hegedus (Wiley, New York, 1987) p. 181.
[6] W.O. Haag, Stud. Surf. Sci. Catal. 84 (1994) 1375.
[7] M. Brandle and J. Sauer, J. Am. Chem. Soc. 120 (1998) 1556.
[8] I.A. Koppel, R.W. Taft, F. Anvia, S.-Z. Zhu, L.-Q. Hu, K.-S. Sung, D.D. Des Marteau, L.M. Yagupolskii, Y.L. Yagupolskii, N.V. Ignat'ev, N.V. Kondratenko, A.U. Volkonskii, V.M. Vlasov, R. Notario and P.-C. Maria, J. Am. Chem. Soc. 116 (1994) 3047.
[9] R.S. Downing, H. van Bekkum and R.A. Sheldon, CATTECH (1997) 95.
[10] T.J. Gricus Kofke and R.J. Gorte, J. Catal. 115 (1989) 233.
[11] K.T. Wan, C.B. Khouw and M.E. Davis, J. Catal. 158 (1996) 311.
[12] A.I. Biaglow, D.J. Parrillo, G.T. Kokotailo and R.J. Gorte, J. Catal. 148 (1994) 213.
[13] R.J. Gorte and A.I. Biaglow, in: *Fluid Cracking Catalysts*, Chemical Industry Series, Vol. 74, eds. M.L. Occelli and P. O'Connor (Dekker, New York, 1997) p. 217.
[14] S.M. Babitz, B.A. Williams, J.T. Miller, R.Q. Snurr, W.O. Haag and H.H. Kung, Appl. Catal. A 179 (1999) 71.
[15] E.P. Parry, J. Catal. 2 (1963) 371.
[16] J.R. Sohn, S.J. Decanio, J.H. Lunsford and D.J. O'Donnell, Zeolites 6 (1986) 225.
[17] J. Klinowski, S. Ramdas, J. Thomas, C.A. Fyfe and J.S. Hartman, J. Chem. Soc. Faraday Trans. II 78 (1982) 1025.
[18] A. Biaglow, D.J. Parrillo and R.J. Gorte, J. Catal. 144 (1993) 193.
[19] R.J. Gorte, Catal. Today 28 (1996) 405.
[20] M.V. Juskelis, J.P. Slanga, T.G. Roberi and A.W. Peters, J. Catal. 138 (1992) 391.
[21] R.J. Gorte, J. Catal. 75 (1982) 164.
[22] R.A. Demmin and R.J. Gorte, J. Catal. 90 (1984) 32.
[23] D.J. Parrillo, C. Lee, R.J. Gorte, D. White and W.E. Farneth, J. Phys. Chem. 99 (1995) 8745.
[24] T.J. Gricus Kofke, R.J. Gorte and W.E. Farneth, J. Catal. 114 (1988) 34.
[25] T.J. Gricus Kofke, R.J. Gorte, G.T. Kokotailo and W.E. Farneth, J. Catal. 115 (1989) 265.
[26] T.J. Gricus Kofke, G.T. Kokotailo and R.J. Gorte, J. Catal. 116 (1989) 252.
[27] J. Tittensor, R.J. Gorte and D. Chapman, J. Catal. 138 (1992) 714.
[28] D.J. Parrillo, A.T. Adamo, G.T. Kokotailo and R.J. Gorte, Appl. Catal. 67 (1990) 107.
[29] C. Pereira and R.J. Gorte, Appl. Catal. A 90 (1992) 145.
[30] A.I. Biaglow, C. Gittleman, R.J. Gorte and R.J. Madon, J. Catal. 129 (1991) 88.
[31] A. Ison and R.J. Gorte, J. Catal. 89 (1984) 150.
[32] M.C. Grady and R.J. Gorte, J. Phys. Chem. 89 (1985) 1305.
[33] M.T. Aronson, R.J. Gorte and W.E. Farneth, J. Catal. 98 (1986) 434.
[34] C.-C. Lee, R.J. Gorte and W.E. Farneth, J. Phys. Chem. B 101 (1997) 3811.
[35] C. Lee, D.J. Parrillo, R.J. Gorte and W.E. Farneth, J. Am. Chem. Soc. 118 (1996) 3262.
[36] C. Pereira and R.J. Gorte, in: *Proceedings of the 9th IZC*, Vol. 2, eds. R. von Ballmoos, J.B. Higgins and M.M.J. Treacy (Butterworths, London, 1993) p. 243.
[37] A.I. Biaglow, R.J. Gorte and D. White, J. Phys. Chem. 97 (1993) 7135.
[38] J. Šepa, C. Lee, R.J. Gorte, D. White, H. Kassab, E. Evleth and M. Allavena, J. Phys. Chem. 100 (1996) 18515.
[39] S. Savitz, A.L. Myers and R.J. Gorte, J. Phys. Chem. B 103 (1999) 3687.
[40] W.P. Fletcher, C.S. Gilbert and A.I. Biaglow, Catal. Lett. 47 (1997) 135.
[41] W.P. Fletcher and A.I. Biaglow, Catal. Lett. 54 (1998) 217.
[42] D.J. Parrillo and R.J. Gorte, Catal. Lett. 16 (1992) 17.
[43] D.J. Parrillo, C. Lee and R.J. Gorte, Appl. Catal. A 110 (1994) 67.
[44] D.J. Parrillo and R.J. Gorte, Thermochim. Acta 312 (1998) 125.
[45] O. Kresnawahjuesa and R.J. Gorte, unpublished data.
[46] J. Šepa, R.J. Gorte, D. White, E. Kassab and M. Allavena, Chem. Phys. Lett. 262 (1996) 321.
[47] A.I. Biaglow, R.J. Gorte and D. White, J. Catal. 148 (1994) 779.
[48] D.H. Aue and M.T. Bowers, *Gas Phase Ion Chemistry*, Vol. 2 (Academic Press, New York, 1979) p. 1.
[49] V.A. Veefkind and J.A. Lercher, Appl. Catal. A 181 (1999) 245.
[50] S. Savitz, A.L. Myers, R.J. Gorte and D. White, J. Am. Chem. Soc. 120 (1998) 5701.
[51] D.J. Parrillo, R.J. Gorte and W.E. Farneth, J. Am. Chem. Soc. 115 (1993) 12441.
[52] A.I. Biaglow, R.J. Gorte and D. White, J. Catal. 150 (1994) 221.
[53] M. Meot-Ner, J. Phys. Chem. 91 (1987) 417.
[54] A.I. Biaglow, J. Šepa, R.J. Gorte and D. White, J. Catal. 151 (1995) 373.
[55] A.I. Biaglow, J. Šepa, R.J. Gorte and D. White, J. Catal. 154 (1995) 208.
[56] J.F. Haw, M.B. Hall, A.E. Alvarado-Swaisgood, E.J. Munson, Z. Lin, L.W. Beck and T. Howard, J. Am. Chem. Soc. 116 (1994) 7308.
[57] J. Šepa, R.J. Gorte, D. White, B.H. Suits and V.S. Swaminathan, in: *Proceedings of the 12th International Zeolite Conference*, eds. M.M.J. Treacy, B.K. Marcus, M.E. Bisher and J.B. Higgins (Materials Research Society, 1998) p. 2287.
[58] M. Allavena and D. White, in preparation.
[59] F. Haase and J. Sauer, J. Am. Chem. Soc. 117 (1995) 3780.
[60] M. Zardkoohi, J.F. Haw and J.H. Lunsford, J. Am. Chem. Soc. 109 (1987) 5278.
[61] M.T. Aronson, R.J. Gorte, W.E. Farneth and D. White, J. Am. Chem. Soc. 111 (1989) 840.
[62] M.T. Aronson, R.J. Gorte and W.E. Farneth, J. Catal. 105 (1987) 455.
[63] J. Kotrla, L. Kubelkova, C.-C. Lee and R.J. Gorte, J. Phys. Chem. B 102 (1998) 1437.
[64] E.G. Derouane, J.M. Andre and A.A. Lucas, J. Catal. 110 (1988) 58.
[65] S. Savitz, F. Siperstein, R.J. Gorte and A.L. Myers, J. Phys. Chem. B 102 (1998) 6865.
[66] J. Šepa, R.J. Gorte, B.H. Suits and D. White, Chem. Phys. Lett. 289 (1998) 281.
[67] R.J. Gorte and D. White, Micropor. Mesopor. Mater., in press.
[68] T.J. Gricus Kofke, Ph.D. thesis, University of Pennsylvania (1989).
[69] J. Šepa, Ph.D. thesis, University of Pennsylvania (1998).